Preprints.org

Article

Not peer-reviewed version

Redox-Active Cerium Fluoride Nanoparticles Mitigate of Double-Stranded DNA Breakage and Modulate Gene Expression Due to Radiation Exposure *In Vitro*

Nikita N. Chukavin , Kristina O. Fillipova , Artem M. Ermakov , Ekaterina E. Karmanova , Nelli R. Popova , Viktoriia A. Anikina , Olga S. Ivanova , Vladimir K. Ivanov , Anton L. Popov *

Posted Date: 7 December 2023

doi: 10.20944/preprints202312.0494.v1

Keywords: cerium fluoride nanoparticles; DNA reparation; double-strand brakes; X-ray radiation

Preprints.org is a free multidiscipline platform providing preprint service that is dedicated to making early versions of research outputs permanently available and citable. Preprints posted at Preprints.org appear in Web of Science, Crossref, Google Scholar, Scilit, Europe PMC.

Copyright: This is an open access article distributed under the Creative Commons Attribution License which permits unrestricted use, distribution, and reproduction in any medium, provided the original work is properly cited.

Preprints (www.preprints.org) | NOT PEER-REVIEWED | Posted: 7 December 2023 doi:10.20944/preprints202312.0494.v1

Disclaimer/Publisher's Note: The statements, opinions, and data contained in all publications are solely those of the individual author(s) and contributor(s) and not of MDPI and/or the editor(s). MDPI and/or the editor(s) disclaim responsibility for any injury to people or property resulting from any ideas, methods, instructions, or products referred to in the content.

Article

Redox-Active Cerium Fluoride Nanoparticles Mitigate of Double-Stranded DNA Breakage and Modulate Gene Expression Due to Radiation Exposure *In Vitro*

Nikita N. Chukavin [1,2], Kristina O. Fillipova [1], Artem M. Ermakov [1,2], Ekaterina E. Karmanova [1], Nelli R. Popova [1], Viktoriia A. Anikina [1], Olga S. Ivanova [3], Vladimir K. Ivanov [4] and Anton L. Popov [1,*]

[1] Institute of Theoretical and Experimental Biophysics of the Russian Academy of Sciences, Pushchino 142290, Moscow Region, Russia; chukavinnik@gmail.com (N.N.C.), kristina.kamensk@mail.ru (K.O.F.), ao_ermakovy@rambler.ru (A.M.E.), silisti@bk.ru (E.E.K.), nellipopovaran@gmail.com (N.R.P.), viktoriya.anikina@list.ru (V.A.A.), runetta05@mail.ru (O.S.I.), antonpopovleonid@gmail.com (A.L.P.)

[2] State University of Education, Moscow, Russia

[3] Frumkin Institute of Physical Chemistry and Electrochemistry of the Russian Academy of Sciences, 119071, Moscow, Russia; runetta05@mail.ru (O.S.I.)

[4] Kurnakov Institute of General and Inorganic Chemistry of the Russian Academy of Sciences, Moscow 119991, Russia; van@igic.ras.ru (V.K.I.)

* Correspondence: antonpopovleonid@gmail.com

Abstract: Ionizing radiation-induced damage in cancer and normal cells leads to apoptosis and cell death, through the intracellular oxidative stress, DNA damage and disorders of their metabolism. Irradiation doses that do not lead to the death of tumor cells can result in the emergence of radioresistant clones of these cells, due to the rearrangement of metabolism and the emergence of new mutations, including those in the genes responsible for DNA repair. The search for the substances capable of modulating the functioning of the tumor cell repair system is an urgent task. Here we analyzed the effect of cerium(III) fluoride nanoparticles (CeF_3 NPs) on normal (human mesenchymal stem cells – hMSCs) and cancer (MCF-7 line) human cells after X-ray radiation. CeF_3 NPs effectively prevent the formation of hydrogen peroxide and hydroxyl radicals in an irradiated aqueous solution, showing pronounced antioxidant properties. CeF_3 NPs are able to protect hMSCs from radiation-induced proliferation arrest, increasing their viability and mitochondrial membrane potential, and, conversely, inducing the cell death of MCF-7 cancer cells, causing radiation-induced mitochondrial hyperpolarization. CeF_3 NPs provided a significant decrease in the number of double-strand breaks (DSBs) in normal cells, while in MCF-7 cells the number of γ-H2AX foci dramatically increased in the presence of CeF_3 4 hours after irradiation. In the presence of CeF_3 NPs, there was a tendency to modulate the expression of most analyzed genes associated with the development of intracellular oxidative stress, cell redox status and the DNA repair system after X ray irradiation. Cerium-containing nanoparticles are capable of providing selective protection of normal cells from radiation-induced injuries and are considered as a platform for the development of promising clinical radioprotectors.

Keywords: cerium fluoride nanoparticles; DNA reparation; double-strand brakes; X-ray radiation

1. Introduction

Ionizing radiation, which is commonly used in cancer therapy, is electromagnetic radiation or photons that ionize the molecules in the cell [1]. Ionized molecules are highly reactive species undergoing a rapid cascade of chemical transformations leading to the breaking of chemical bonds [2]. As a result, the DNA structure, the main target of ionizing radiation, is disrupted, and highly

© 2023 by the author(s). Distributed under a Creative Commons CC BY license.

Preprints (www.preprints.org) | NOT PEER-REVIEWED | Posted: 7 December 2023 doi:10.20944/preprints202312.0494.v1

reactive products are formed from water molecules contained in the cell, such as reactive oxygen species (ROS) and free radicals [3]. Consequently, exposure to ionizing radiation directly and indirectly leads to a damage to the basic structures of the cell and its death. However, ionizing radiation also triggers a series of signaling cascades that promote cell survival and activate cellular processes such as DNA repair, cell cycle arrest and autophagy, which leads to radioresistance and the development of tumor cell adaptability [4].

Selective increase of radiosensitivity of tumor cells is one of the important tasks of the development of a new modern treatment methods of solid tumors radiation therapy [5]. There are a few approaches to increase the radiation sensitivity of cancer cells, starting with increasing the level of tumor tissue oxygenation, ending with the use of kinase inhibitors (for example, PI3K-like kinases) or cell cycle checkpoints [6]. The most promising agents for these purposes is the use of nanoradiosensitizers based on high Z elements, which can effectively accumulate in tumor cells and locally enhance the radiation dose, thereby increasing the damaging effect of ionizing radiation [7]. Some of them have already been approved by the FDA or are at various stages of clinical trials [8,9]. Thus, the use of nanoscale particles with a good biosafety profile and the ability to effectively absorb ionizing radiation is a promising strategy in the development of new effective radiosensitizers.

Fluoride nanoparticles have their unique physicochemical properties, which determines such interest in the study. In particular, lanthanide fluorides (LnF_3, Ln = lanthanides) have very low solubility (about 10^{-5}–10^{-6} mol/L) [10] and, as a consequence, low toxicity [11]. For example, previous studies *in vivo* on planarians confirm that CeF_3 nanoparticles have low toxicity at concentrations of 1 μM - 10 mM [12]. Cerium fluoride is one of the best scintillators for use in biomedicine [13]. Scintillators are compounds that are capable of emitting photons when they absorb ionizing radiation of various types, including X rays. CeF_3 NPs is an effective scintillator, since when irradiated with X-rays, it emits UV light due to fluorescence at a wavelength of 325 nm. In the nanoscale state, cerium ions are able to transfer excitation energy to ions in its doped crystal lattice, for example, rare-earth ions of other metals (for example, europium or terbium) located in the crystal lattice [14]. In [15], the cytotoxicity of Ce^{3+}, Tb^{3+}: $NaYF_4$ spherical particles against Capan-1 cells with a size of 16.7 nm was studied in the concentration range of 0.5 pM - 40 nM using the MTT assay. After 48 h of incubation, a dose-dependent linear decrease in viability was detected from ~100% at 0.5 pM to ~30% at 40 nM. According to the general opinion, cerium-containing nanoparticles with a predominant content of cerium in the trivalent state on the surface provide their SOD-mimetic activity [16]. Trivalent cerium ions determine the redox-dependent anti-apoptotic effect. For example, PEGylated CeO_2 nanoparticles with high Ce^{3+} content protect cells from ROS-induced cell death *in vitro* and reduce the rate of ischemic cell death *in vivo* [17]. Soh et al. synthesized 2 nm cerium zirconium oxide ($Ce_{0.7}Zr_{0.3}O_2$) nanoparticles with a high concentration of Ce^{3+} ions, which demonstrated anti-inflammatory activity in two representative models of sepsis [18]. In addition, both undoped and terbium-doped CeF_3 nanoparticles have been shown to provide effective cell protection against vesicular stomatitis virus [11]. CeF_3 NPs were shown to prevent oxidative discoloration of indigo carmine dye induced by exposure to hydrogen peroxide, where a dose-dependent protective effect was detected. Luminescent nanocrystals containing lanthanide Ln^{3+} ions are currently of interest to researchers because of their unique characteristics, including a long luminescence lifetime, high resistance to photochemical decomposition and photobleaching, as well as high chemical and physical stability [19–21]. In addition, these nanocrystals have the ability to form stable colloids [22]. CeF_3:Tb@LaF_3 based nanomaterials are promising biomedical agents due to their high colloidal stability and resistance to photobleaching [23,24]. Coating of CeF_3:Tb^{3+} NPs with LaF_3 shells improves the emission intensity by more than 25% compared to conventional CeF_3:Tb^{3+} nanoparticles. Energy losses from the surface luminescence centers were significantly reduced due to the LaF_3 shell, which served as a barrier for energy transfer to the upper surface of the shell, and therefore the lifetime and luminescence intensity of these nanoparticles significantly increased [25]. The luminescent and magnetic properties of lanthanide nanoparticles may be of fundamental importance in the development of multifunctional nanomaterials, allowing them to be used in MRI and other luminescence methods [26,27]. CeF_3 NPs can be considered as an effective platform for development

Preprints (www.preprints.org) | NOT PEER-REVIEWED | Posted: 7 December 2023 doi:10.20944/preprints202312.0494.v1

of promising redox-active drugs that can find their application in the therapy and diagnosis of oncological diseases.

In this work, redox-active CeF_3 NPs were used to analyze their impact to cell proliferation, mitochondrial membrane potential and DNA repair process upon X-ray irradiation. The effect CeF_3 NPs on the rate of DSBs in normal and cancer cells was analyzed and the possible molecular mechanisms of this effect were discussed. The significant improvement of the DSBs DNA repair rate by CeF_3 NPs in normal cells exposed to ionizing radiation shows new opportunities in development of advanced radiation-mediated cancer therapies.

2. Materials and Methods

2.1. Synthesis and characterization of CeF_3 NPs

CeF_3 NPs were synthesized by precipitation in alcoholic media [11]. UV–vis absorption spectra of the colloid solution was recorded using standard quartz cells for liquid samples on a UV5 Nano spectrophotometer (Mettler Toledo, USA). Transmission electron microscopy and selected area electron diffraction (SAED) analysis was performed using a Leo 912 AB Omega electron microscope operating at 100 kV acceleration voltage. Nanoparticle size measurements by dynamic light scattering and zeta-potential were carried out on a BeNano Zeta particle size analyzer (BetterSize, China). Powder X-ray diffraction analysis (XRD) of CeF_3 NPs sol (dried at 40°C) was performed using a Bruker (Billerica, MA, USA) D8 Advance diffractometer (CuKα radiation), in the angle range of 20-90°2 Θ, with a step of 0.02°2Θ and a signal acquisition time of 0.4 s per step. Full-profile analysis of XRD patterns was performed using TOPAS v.4.2 software (Billerica, MA, USA) and diffraction maxima were fitted to Voigt pseudo-functions.

2.2. Cell cultures

The experiments were performed using a culture of human mesenchymal stem cells (hMSc) derived from the third molar bud, extracted from a healthy 12-year-old patient for orthodontic indications, and MCF-7 human breast cancer cell line, obtained from Theranostics and Nuclear Medicine Laboratory cryostorage (ITEB RAS, Pushchino, Russia). The *in vitro* experiments were performed in agreement with good clinical practice and the ethical principles of the current edition of the Declaration of Helsinki, after the permission of the Ethics Committee of Institute of Theoretical and Experimental Biophysics of the Russian Academy of Sciences (Pushchino, Moscow region, Russian Federation), protocol No. 35 from 5 March 2022. Postnatal human dental pulp stem cells were extracted from the third molar tooth of a human donor (of an 12-year-old donor). The tooth was removed according to the orthodontic indications of the dental clinic «Dr. MUN» (Moscow, Russia), in accordance with the ethics committee, after consent was signed by the patient's parents. The cells were cultivated in a DMEM/F12 (1:1) medium containing 10% of fetal bovine serum (FBS), 50 μg/mL of penicillin, 50 μg/mL of streptomycin and 1% of l-glutamine, at 37 °C in a humid atmosphere, comprising 95% air and 5% CO_2. The cells were seeded at a density of 20,000–35,000/cm^2. The medium was replaced by a medium containing CeF_3 NPs in different concentrations (10^{-3} –10^{-7} M) 6 h after cell attachment. In the control experiments, the cells were cultured without CeF_3 NPs.

2.3. X-ray irradiation

X-ray irradiation of the cell cultures was performed using an X-ray therapeutic machine RTM-15 (Mosrentgen, Russia) in a dose of 1 and 5 Gy for CeF_3 NPs solution, 15 Gy for cell cultures, 1.5 Gy for DSBs analysis at a dose rate of 1 Gy/min, 200 kV voltage, 37.5 cm focal length and a 20 mA current.

2.4. Assessment of CeF_3 NPs antioxidant activity

To evaluate the antioxidant activity of CeF_3 NPs, we determined the concentration of hydrogen peroxide after X-ray irradiation of CeF_3 NPs by enhanced chemiluminescence using a luminol – 4-iodophenol – peroxidase system [28]. We used TRIS buffer to maintain constant pH 7.2. The

Preprints (www.preprints.org) | NOT PEER-REVIEWED | Posted: 7 December 2023 doi:10.20944/preprints202312.0494.v1

irradiation dose was 5 Gy (1 Gy per min). A liquid scintillation counter Beta-1 (MedApparatura, Ukraine), operating in the mode for counting single photons (with one photomultiplier and the coincidence scheme disengaged), was used as a highly sensitive chemiluminometer. The high sensitivity of this method allows registering H_2O_2 at a concentration of < 1 nM. The H_2O_2 content was determined using calibration dependencies of chemiluminescence on H_2O_2 concentration in the solution. The concentration of H_2O_2 used for the calibration was determined spectrophotometrically at 240 nm using a molar absorption coefficient of 43.6 $M^{-1} \times cm^{-1}$. The hydroxyl radical under X-ray irradiation was measured using coumarin-3-carboxylic acid [29]. The fluorescence intensity of hydroxylated coumarin-3-carboxylic acid (ex 395/em 450 nm) was measured on a Cary Eclipse spectrofluorimeter (Agilent, Australia) at room temperature.

2.5. Cell proliferation analysis

The cell growth analysis after incubation with CeF_3 NPs and X-ray irradiation was estimated by counting the number of the cells stained with Hoechst 33342 using fluorescent imager Zoe® (BioRAd, USA). At least four measurements were made for each CeF_3 NPs (10^{-3}-10^{-7} M). The data are presented as growth curves (mean with SD).

2.6. Analysis of DNA double-strand breaks by γ-H2AX foci

Cells were seeded in 35 mm Petri dishes with a central hole (Ibidi, Germany). After X ray irradiation the cells were washed twice with phosphate-buffered saline (PBS, 3.2 mM Na_2HPO_4, 0.5 mM KH_2PO_4, 1.3 mM KCl, 135 mM NaCl, pH 7.4). Then the cells were fixed with 4 % paraformaldehyde in PBS for 15 min, permeabilized with 0.1 % Triton X-100 in PBS for 5 min, washed extensively with PBS and blocked in 5% BSA in PBS (Gibco, Invitrogen, Karlsruhe, Germany) for 30 min at room temperature (RT). The primary antibodies, monoclonal mouse γH2AX (ab195188 Recombinant, Anti-gamma H2A.X (phospho S139), (Alexa Fluor® 488), Abcam) were used for immunostaining. Image acquisition of the DSBs was performed using an inverted fluorescent microscopy Zeiss Axiovert Observer 200 (Carl Zeiss Microscopy, Jena, Germany). Analysis of γH2AX stained cells was performed with an optional manual correction in individual cells. For each experimental group, at least 200 cells were analyzed. Image J software was used to quantify the detected γH2AX foci.

2.7. RT-PCR (Genes expression analysis)

Reverse transcription was performed with a Evrogen kit (Russia, Moscow), using an oligodT primer according to the manufacturer's protocol. For PCR reaction, a mixture was used with SYBR Green dye (Evrogen, Russia). To conduct a PCR-RT analysis, a BioRad CFX-96 amplifier Real-Time PCR System was used. The expression of 96 genes responsible for key cell processes under oxidative stress was thus determined (Table S1). For PCR profiling, the genes to be analyzed were selected from the database http://www.sabiosciences.com/. The level of gene transcription was normalized by the levels of expression of housekeeping genes β-actin, rplp0 (ribosomal protein, large, P0) and GAPDH (glyceraldehyde-3-phosphate dehydrogenase). The gene-specific primers were prepared using Genesis software. Each measurement was made twice (internal repetition) and averaged for two independent samples. A sample without a reverse transcription stage was used as the control. The expression data obtained were analyzed using online services http://www.sabiosciences.com/, mayday-2.14 software (Center for Bioinformatics, Tübingen, Germany) and Genesis software.

2.8. Statistical analysis

The experiments were conducted in 3–4 repetitions, with three independent repetitions for each CeF_3 NPs concentration. Experimental results were compared with untreated control. Statistical analysis was performed using the methods of variation statistics (ANOVA, Student's *t*-test.). The mean values and the standard deviation (SD) of the mean were determined. The obtained data were processed using the GraphPad 8.0 Software.

Preprints (www.preprints.org) | NOT PEER-REVIEWED | Posted: 7 December 2023 doi:10.20944/preprints202312.0494.v1

3. Results and Discussion

The synthetic procedures resulted in stable aqueous sol of highly crystalline CeF_3 NPs. Selected area electron diffraction patterns of the samples (Figure 1a) correspond to the *P6_3/mcm* space groups for hexagonal CeF_3 structure. High crystallinity of CeF_3 NPs synthesized using soft chemistry routes is typical for this Ce(III)-containing material [11]. According to XRD results, the resulting sol contains as a dispersed phase pure hexagonal cerium fluoride (sp. gr. P63/mcm) with a crystallite size of 24 ± 2 nm(Figure 1b). ζ-potential of CeF_3 NPs sol equals +41 mV, corroborating its high stability (Data not presented). The hydrodynamic radii of CeF_3 NPs in the sol diluted with distilled water was 40±2 nm (Figure 1c), indicating the low degree of the particle agglomeration. According to TEM data, the size of CeF_3 NPs was 15–25 nm. The nanoparticles possess notable faceting, which indicates high degree of crystallinity. Highly crystalline CeF_3 NPs is expected to contain only trivalent cerium [30,31]. The main UV absorption peak of CeF NPs is located at 250 nm (Figure 1d). According to literature data, UV absorption spectra of Ce^{3+} ions have a maximum at 253.6 nm with a molar extinction coefficient of 685 M^{-1} cm^{-1} [32]. Data presented in Figure 1e shows that CeF_3 NPs are capable of preventing the formation of hydrogen peroxide in water upon X-ray exposure due to their catalase-like properties. CeF_3 NPs at a concentration of 10^{-7} M do not lead to a decrease in the level of hydrogen peroxide formed after irradiation of the solution. An increase in the concentration of CeF_3 NPs to 10^{-6} M provides a pronounced antioxidant effect, which is expressed in a significant (up to 30%) decrease in the concentration of hydrogen peroxide. CeF_3 NPs at a concentration of 10^{-5} M reduced the level of hydrogen peroxide after irradiation to zero values. A possible explanation for such CeF_3 NPs catalase-like activity can be explained by the number of binding sites for hydrogen peroxide, which directly correlates with the nanoparticle size. Catalytic decomposition of hydrogen peroxide is a heterogeneous process that occurs at the interface and depends on the specific surface area. CeF_3 NPs have a size of 15-25 nm, which corresponds to ≈ 10% of surface cerium atoms [33,34]. Thus, the specific surface area of a CeF_3 NPs occupies a smaller part of its entire surface. CeF_3 NPs reduce the concentration of hydroxyl radical (Figure 1f), which is formed during irradiation only in high concentrations (10^{-5} M).

Preprints (www.preprints.org) | NOT PEER-REVIEWED | Posted: 7 December 2023 doi:10.20944/preprints202312.0494.v1

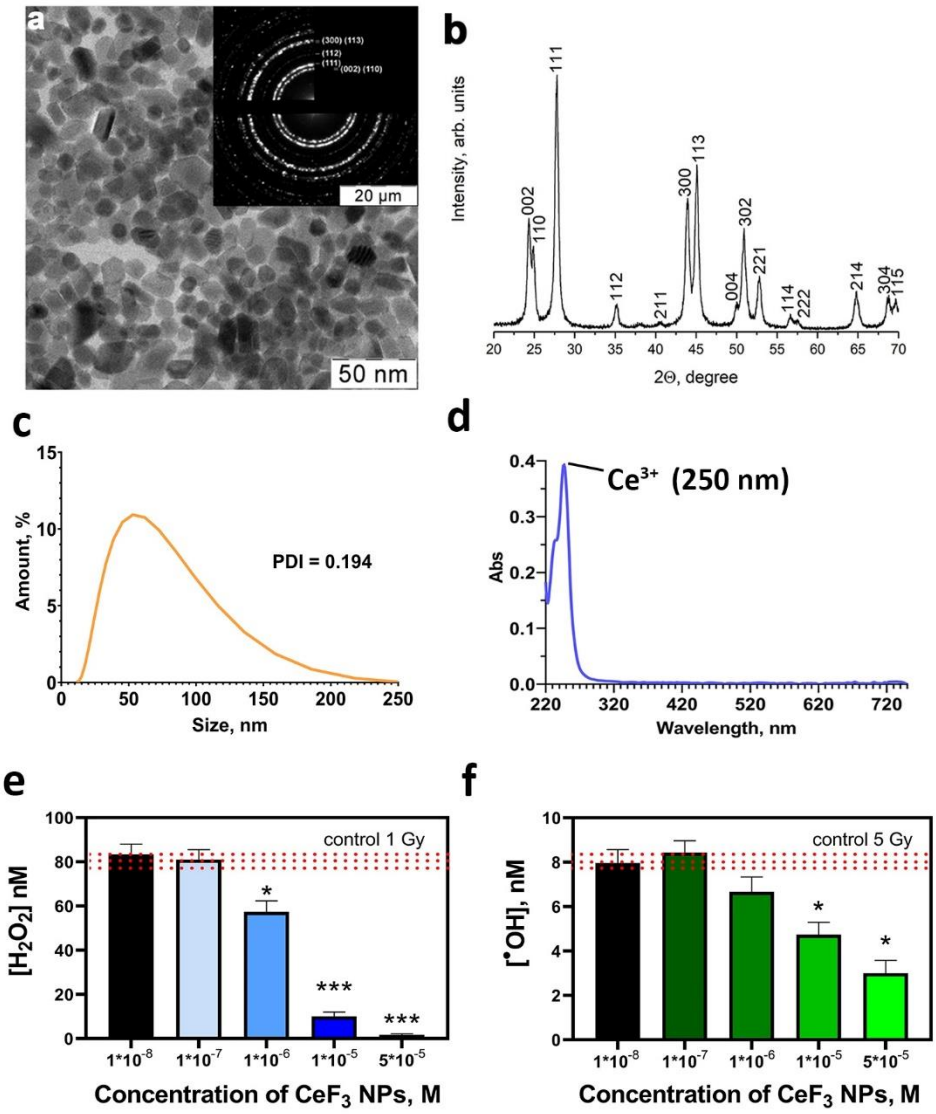

Figure 1. The TEM image (a), XRD (b), hydrodynamic radii distribution (c) and UV spectra (d) of CeF_3 NPs; Hydrogen peroxide(e) and hydroxyl radicals(f) formation induced by X-ray irradiation in a solution, containing CeF_3 NPs. Insets in Figure 1a show selected area electron diffraction data.

CeF_3 NPs selectively modulate the proliferative activity of normal and tumor cells (Figure 2). Preincubation of hMSCs with CeF_3 NPs leads to an increase in their proliferative activity (Figure 2a,b). Irradiation of hMSCs leads to inhibition of proliferative activity (reduction to 40% relative to non-irradiated control), however, cell pretreatment with CeF_3 NPs ensures the preservation of positive dynamics of proliferative activity at concentrations (10^{-3}-10^{-4} M), which confirms the pronounced radioprotective effect. At the same time, the proliferative activity of tumor cells significantly decreases in the presence of CeF_3 NPs on the 5th day of coincubation, and X ray irradiation (15 Gy dose) enhances this effect (Figure 2c,d). Thus, CeF_3 NPs, on the one hand, stimulate the proliferative activity of normal cells, and, on the other, suppress the proliferative activity of tumor cells and have a radiosensitizing effect on them. Presumably, the above-described biological activity of CeF_3 NPs can be realized by their effect on the modulation of various intracellular molecular cascades that differ in normal and tumor cells.

Preprints (www.preprints.org) | NOT PEER-REVIEWED | Posted: 7 December 2023 doi:10.20944/preprints202312.0494.v1

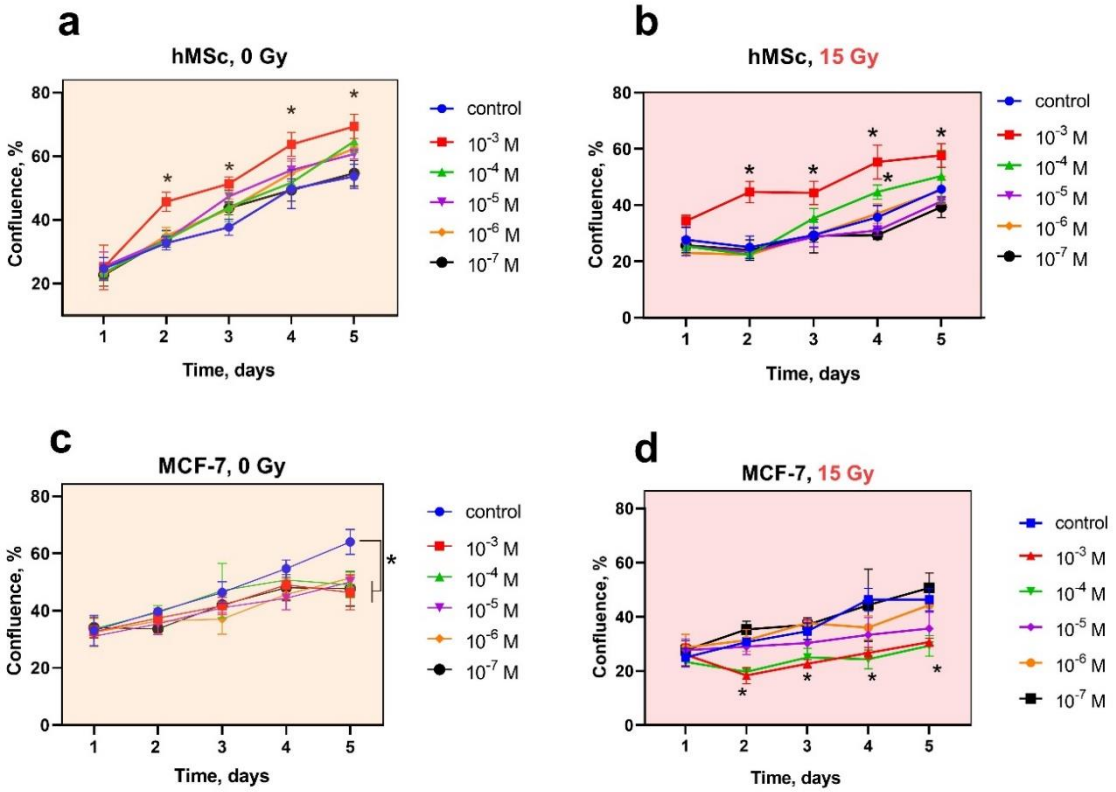

Figure 2. The cell proliferation analysis of hMSc and MCF-7 cell lines after X-ray irradiation with CeF_3 NPs. The hMSc and MCF-7 cells were overnight pretreated with CeF_3 NPs (10^{-3} – 10^{-7} M) and then irradiated with 15 Gy of X-rays. The change in the confluence of cell cultures was observed for 5 days. Significant differences compared with untreated control using the t-test, * $p < 0.05$.

The effect of ionizing irradiation on eukaryotic cells leads to disruption of the electron transport chain system in mitochondria, which leads to delayed radiation-induced MMP collapse and increased generation of reactive oxygen species (ROS) [35,36]. Increased generation of ROS in mitochondria and a decrease in ATP synthesis in irradiated cells can be observed for a long time [37]. Thus, damaged mitochondria become inducers of oxidative stress over a long period of time. Using the cationic dye tetramethylrhodamine (TMRE), which accumulates in mitochondria in a voltage-dependent manner, we analyzed the mitochondrial membrane potential **(**MMP) of cell cultures 72 hours after irradiation (Figure 3). It was revealed that irradiation of hMSCs at a dose of 15 Gy does not lead to a significant decrease in MMP (Figure 3a). Pretreatment of cells with CeF_3 NPs also does not affect the MMP level after irradiation. It is worth noting that after irradiation we observe morphological changes, in particular, the enlargement of mitochondria, which confirms the development of the senescence process. Pretreatment of cancer cells with CeF_3 NPs leads to a slight decrease in the level of MMP, but no statistically significant decrease is observed. Irradiation of tumor cells leads to hyperpolarization of mitochondria (increase in MMP), and their pretreatment with CeF_3 NPs nanoparticles only enhances this effect in a dose-dependent manner (Figure 3b). Thus, the combined effect of CeF_3 NPs and X-ray irradiation have exactly the opposite effect on the mitochondrial membrane potential of tumor cells.

Preprints (www.preprints.org) | NOT PEER-REVIEWED | Posted: 7 December 2023 doi:10.20944/preprints202312.0494.v1

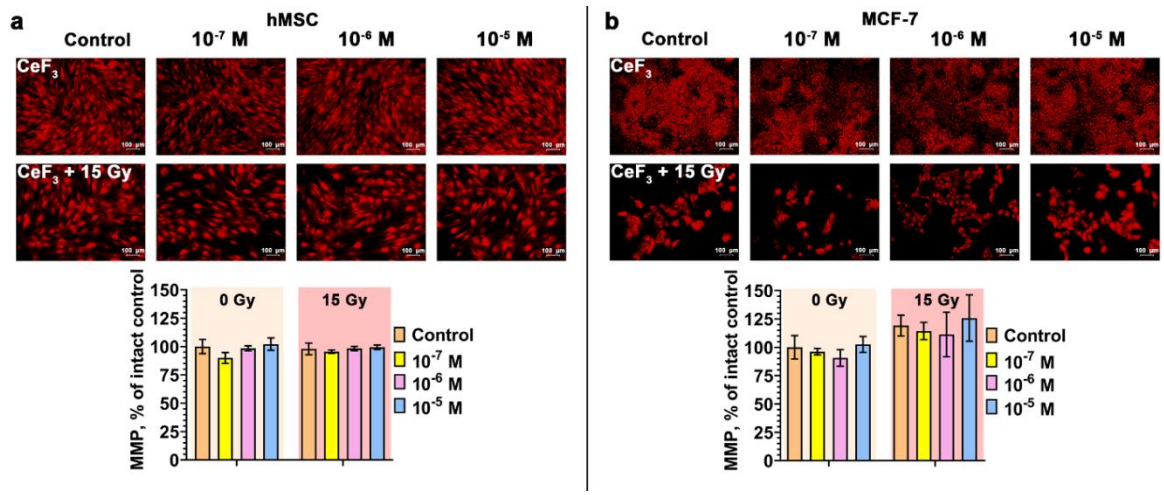

Figure 3. Mitochondrial membrane potential (MMP) of hMSCs and MCF-7 cells 72 hours after X-ray irradiation (15 Gy dose) with CeF_3 NPs in various concentrations (10^{-7}-10^{-5} M). The MMP of cells are indicated as the mean with standard deviation (SD) (n=3).

Ionizing radiation generally leads to diverse DNA damages, including single-strand and double-strand breaks [3]. Double-strand breaks (DSBs) make up a small part of such damage, while it is their number that is decisive for the further fate of the cell including the cell cycle arrest, DNA repair processes activation or apoptosis triggering [38]. Using γ-H2AX histone staining with FITC-labeling antibodies, we evaluated the dynamics of the DSBs repair in normal and cancer cells after irradiation. Figure 4 shows that the number of double-strand breaks significantly reduced in the presence of CeF_3 NPs in both normal (hMSCs) and cancer (MCF-7) cells 1 hour after irradiation. Then, after 4 hours of incubation, the dynamics of the repair of DSBs become different for normal and cancer cells. For normal cells, the protective effect of CeF_3 NPs is observed for all CeF_3 NPs concentrations, which is expressed in a decrease in the number of DSBs (Figure 4 a, c). Meanwhile, for MCF-7cancer cells, there is a significant increase of DSBs in comparison with the irradiated control (Figure 4 b, d).

Preprints (www.preprints.org) | NOT PEER-REVIEWED | Posted: 7 December 2023 doi:10.20944/preprints202312.0494.v1

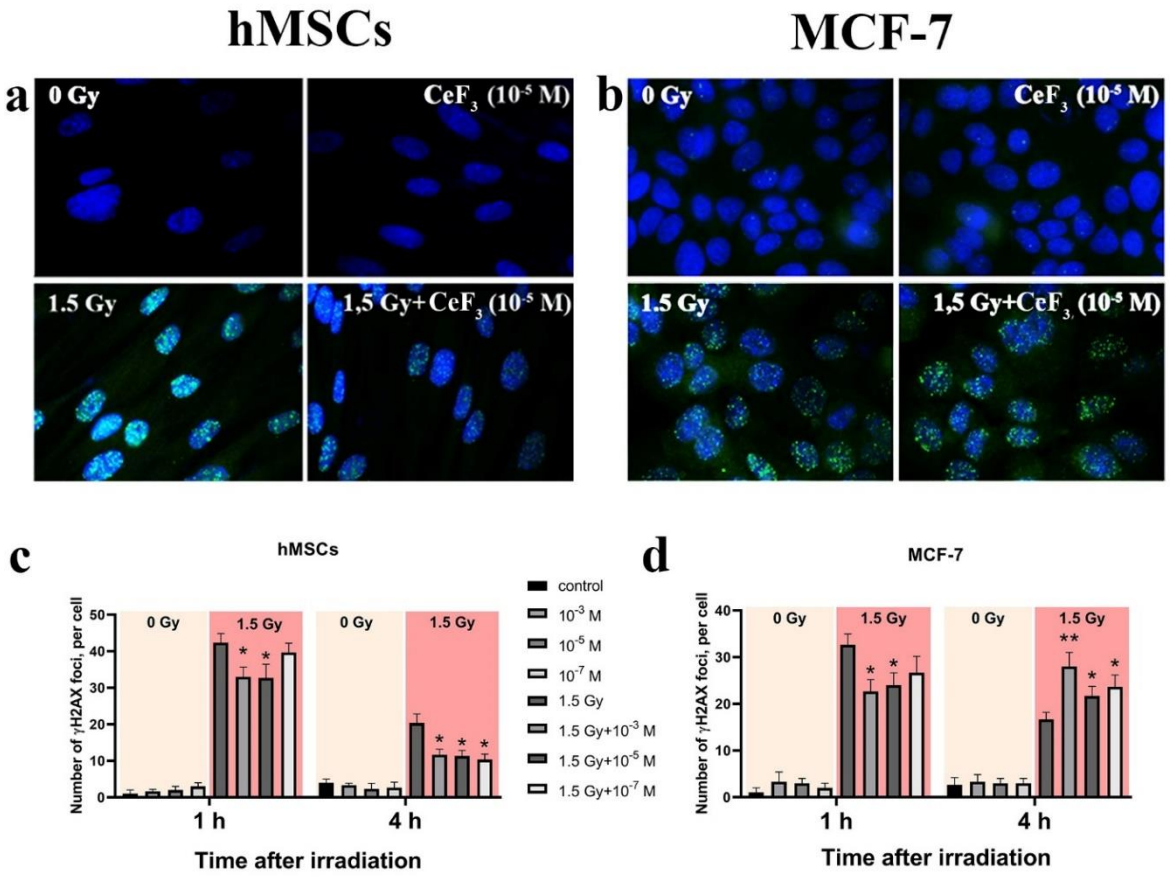

Figure 4. Radiation-induced γ-H2AX foci determined using FITC-labeled antibody by fluorescent microscopy (a, b). Quantitative analysis of DSBs repair process 1 h or 4 h after irradiation (c, d). The hMSc and MCF-7 cells were pretreated with CeF_3 NPs irradiated with 1,5 Gy of X-rays and let to recover for 1 h or 4 h post irradiation. Data points represent means of two experiments, at least 200 cells were counted at each treatment condition (b). Unirradiated cells (0 Gy) were used as control. Data presented as mean of γ-H2AX foci per cell ±SD, n=200. Statistically significant differences are indicated by the * ($p<0,05$).

The effect of CeF_3 NPs on the expression pattern in both cancer (MCF-7) and normal (hMSc) cells revealed downregulation of most genes (49 out of 89) (Figure 5). For example, genes coding some members of the glutathione peroxidase family (GPX1, GPX2, GPX5) were significantly down-regulated. Irradiation of MCF-7 cells in the presence of CeF_3 NPs revealed upregulation in 13 genes, as well as suppressed expression of 17 studied genes. PCA analysis revealed a clear effect of radiation on the pattern of gene expression, and its pronounced modulation in the presence of CeF_3 NPs. It should be noted that the separate action of irradiation or CeF_3 NPs similarly influenced the expression patterns for both types of cell cultures, while the combined action of CeF_3 NPs and X-ray irradiation was fundamentally different for cancer and normal cells. This difference can be associated with the effect of CeF_3 NPs on the signaling pathways of the cell, in particular, on NF-κB. NF-κB is a transcription factor that participates in the regulation of various physiological processes, including response to oxidative stress, inflammation and apoptosis [39]. The activation mechanisms of NF-κB pathway are associated with inhibition of IκB subunit. Earlier, it has been shown that CeO_2 NPs decrease intracellular oxidative stress and suppress phosphorylation of IκBα and the translocation of P65 subunits of NF-κB into the cell nuclei, which provide cell protection under cigarette smoke exposure [40].

Preprints (www.preprints.org) | NOT PEER-REVIEWED | Posted: 7 December 2023 doi:10.20944/preprints202312.0494.v1

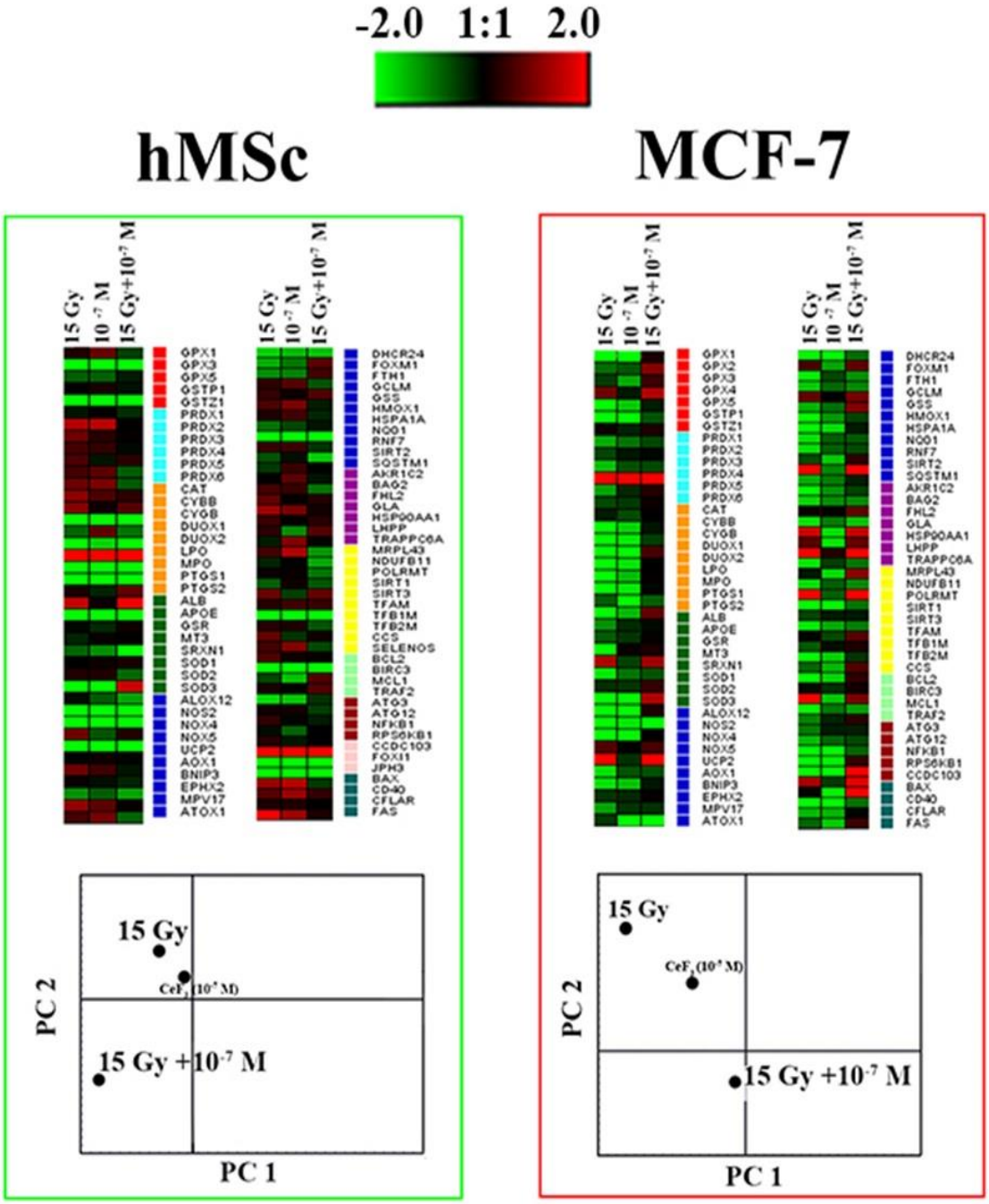

Figure 5. Heat map of gene expression in hMSc (a) and MCF-7 (b) cells treated with CeF_3 NPs (10^{-7} M). The intensity scale of the standardized expression values ranges from -3 (green: low expression) to +3 (red: high expression), with the 1:1 intensity value (black) representing the control (non-treated cells). Principal component analysis (PCA) data is presented under heat map.

Thus, we hypotized that CeF_3 NPs are able to modulate the activity of NF-κB both in the direction of activation and in the direction of suppression. NF-κB signaling pathway is also responsible for the repair of DSBs after X ray exposure [41]. In cancer cell (MCF-7 cells), inhibition of the IKK-NFκB pathway by a specific inhibitor of IKKβ was found to significantly reduce the repair rate of irradiation-induced DSBs and sensitized MCF-7 cells to clonogenic cell death. Recent studies show that CeO_2 NPs are able to influence key cell signaling pathways, regulating the processes of proliferation, apoptosis, differentiation, protein synthesis and cell cycle progression [42]. Thus, the study of cerium-containing nanoparticles effect on cell signaling pathways could be one of the ways

Preprints (www.preprints.org) | NOT PEER-REVIEWED | Posted: 7 December 2023 doi:10.20944/preprints202312.0494.v1

to increase the sensitization of cancer cells to ionizing radiation, increasing the efficiency of radiation therapy of oncological diseases.

5. Conclusions

CeF_3 NPs significantly reduce the content of hydrogen peroxide and hydroxyl radicals after X-ray exposure. CeF_3 NPs in normal cells act as a proliferation stimulator and a radioprotector reducing the number of DSBs, maintaining high viability, proliferative activity and mitochondrial membrane potential maintaining viability, proliferative activity and mitochondrial membrane potential close to control values after irradiation. Meanwhile, in cancer cells CeF_3 NPs act as proliferation suppressor and a radiosensitizer, which slows down the rate of DSBs repair 4 h after irradiation. CeF_3 NPs reduce the proliferative activity of cancer cells, lead to radiation-induced hyperpolarization of mitochondria. The molecular mechanisms of the selective action of CeF_3 NPs are most likely associated with the modulation of intracellular signaling pathways through the regulation of the redox status of the cell which we confirmed by RT-PCR analysis. The observed selective enhancement of DSBs repair process of cerium-containing nanoparticles can be used to increase the sensitization of cancer cells in a patient during radiation therapy and to protect healthy tissues in the immediate vicinity of the tumor.

Supplementary Materials: The following supporting information can be downloaded at the website of this paper posted on Preprints.org. Table S1. The estimation of the genes expression in cultured cells by the method of the real time (RT) PCR, and the primers used in the study.

Author Contributions: Conceptualization, A.L.P. and V.K.I; methodology, N.N.C.; investigation N.N.C., A.L.P., K.O.F., A.E.M., E.E.K., N.R.P., V.A.A., O.S.I.; data curation, A.L.P.; writing—original draft preparation, A.L.P., N.N.C., V.K.I.; writing—review and editing, A.L.P., V.K.I.; visualization, N.N.C.; supervision, A.L.P.; project administration, A.L.P.; funding acquisition, A.L.P. All authors have read and agreed to the published version of the manuscript.

Funding: This research was funded by the Ministry of Science and Higher Education of the Russian Federation for Institute of Theoretical and Experimental Biophysics of the Russian Academy of Sciences (State Assignment № 075-01025-23-01).

Institutional Review Board Statement: The *in vitro* experiments were performed in agreement with good clinical practice and the ethical principles of the current edition of the Declaration of Helsinki, after the permission of the Ethics Committee of Institute of Theoretical and Experimental Biophysics of the Russian Academy of Sciences (Pushchino, Moscow region, Russian Federation), protocol No. 35 from 5 March 2022. Postnatal human dental pulp stem cells were extracted from the third molar tooth of a human donor (of an 12-year-old donor). The tooth was removed according to the orthodontic indications of the dental clinic «Dr. MUN» (Moscow, Russia), in accordance with the ethics committee, after consent was signed by the patient's parents. All the experiments were carried out in agreement with good clinical practice and the ethical principles of the current edition of the Declaration of Helsinki.

Informed Consent Statement: Informed consent was obtained from all subjects involved in the study.

Acknowledgments: We express our gratitude to Shcherbakov A.B. for discussion of the experimental results.

Conflicts of Interest: The authors declare no conflict of interest.

References

1. Baskar, R.; Lee, K.A.; Yeo, R.; Yeoh, K.-W. Cancer and Radiation Therapy: Current Advances and Future Directions. Int J Med Sci **2012**, 9, 193–199, doi:10.7150/ijms.3635.
2. Phaniendra, A.; Jestadi, D.B.; Periyasamy, L. Free Radicals: Properties, Sources, Targets, and Their Implication in Various Diseases. *Indian J Clin Biochem* **2015**, *30*, 11–26, doi:10.1007/s12291-014-0446-0.
3. Borrego-Soto, G.; Ortiz-López, R.; Rojas-Martínez, A. Ionizing Radiation-Induced DNA Injury and Damage Detection in Patients with Breast Cancer. *Genet Mol Biol* **2015**, *38*, 420–432, doi:10.1590/S1415-475738420150019.
4. Zhang, D.; Tang, B.; Xie, X.; Xiao, Y.-F.; Yang, S.-M.; Zhang, J.-W. The Interplay between DNA Repair and Autophagy in Cancer Therapy. *Cancer Biol Ther* **2015**, *16*, 1005–1013, doi:10.1080/15384047.2015.1046022.

Preprints (www.preprints.org) | NOT PEER-REVIEWED | Posted: 7 December 2023 doi:10.20944/preprints202312.0494.v1

5. Elsaid, M.Y.; Shahi, A.; Wang, A.R.; Baiu, D.C.; Li, C.; Werner, L.R.; Singhal, S.; Hall, L.T.; Weichert, J.P.; Armstrong, E.A.; et al. Enhanced Radiosensitivity in Solid Tumors Using a Tumor-Selective Alkyl Phospholipid Ether Analog. *Molecular Cancer Therapeutics* **2018**, *17*, 2320–2328, doi:10.1158/1535-7163.MCT-17-0897.
6. Moding, E.J.; Kastan, M.B.; Kirsch, D.G. Strategies for Optimizing the Response of Cancer and Normal Tissues to Radiation. *Nat Rev Drug Discov* **2013**, *12*, 526–542, doi:10.1038/nrd4003.
7. Hu, Y.; Paris, S.; Barsoumian, H.; Abana, C.O.; He, K.; Wasley, M.; Younes, A.I.; Masrorpour, F.; Chen, D.; Yang, L.; et al. Radiation Therapy Enhanced by NBTXR3 Nanoparticles Overcomes Anti-PD1 Resistance and Evokes Abscopal Effects. *Int J Radiat Oncol Biol Phys* **2021**, *111*, 647–657, doi:10.1016/j.ijrobp.2021.06.041.
8. Bagley, A.F.; Ludmir, E.B.; Maitra, A.; Minsky, B.D.; Li Smith, G.; Das, P.; Koong, A.C.; Holliday, E.B.; Taniguchi, C.M.; Katz, M.H.G.; et al. NBTXR3, a First-in-Class Radioenhancer for Pancreatic Ductal Adenocarcinoma: Report of First Patient Experience. *Clin Transl Radiat Oncol* **2022**, *33*, 66–69, doi:10.1016/j.ctro.2021.12.012.
9. Verry, C.; Dufort, S.; Villa, J.; Gavard, M.; Iriart, C.; Grand, S.; Charles, J.; Chovelon, B.; Cracowski, J.-L.; Quesada, J.-L.; et al. Theranostic AGuIX Nanoparticles as Radiosensitizer: A Phase I, Dose-Escalation Study in Patients with Multiple Brain Metastases (NANO-RAD Trial). *Radiother Oncol* **2021**, *160*, 159–165, doi:10.1016/j.radonc.2021.04.021.
10. Pudovkin, M.S.; Zelenikhin, P.V.; Shtyreva, V.; Morozov, O.A.; Koryakovtseva, D.A.; Pavlov, V.V.; Osin, Y.N.; Evtugyn, V.G.; Akhmadeev, A.A.; Nizamutdinov, A.S.; et al. Coprecipitation Method of Synthesis, Characterization, and Cytotoxicity of Pr^{3+}:LaF_3 (C_{Pr} = 3, 7, 12, 20, 30%) Nanoparticles. *Journal of Nanotechnology* **2018**, *2018*, e8516498, doi:10.1155/2018/8516498.
11. Shcherbakov, A.B.; Zholobak, N.M.; Baranchikov, A.E.; Ryabova, A.V.; Ivanov, V.K. Cerium Fluoride Nanoparticles Protect Cells against Oxidative Stress. *Materials Science and Engineering: C* **2015**, *50*, 151–159, doi:10.1016/j.msec.2015.01.094.
12. Ermakov, A.; Popov, A.; Ermakova, O.; Ivanova, O.; Baranchikov, A.; Kamenskikh, K.; Shekunova, T.; Shcherbakov, A.; Popova, N.; Ivanov, V. The First Inorganic Mitogens: Cerium Oxide and Cerium Fluoride Nanoparticles Stimulate Planarian Regeneration via Neoblastic Activation. *Materials Science and Engineering: C* **2019**, *104*, 109924, doi:10.1016/j.msec.2019.109924.
13. Clement, S.; Deng, W.; Camilleri, E.; Wilson, B.C.; Goldys, E.M. X-Ray Induced Singlet Oxygen Generation by Nanoparticle-Photosensitizer Conjugates for Photodynamic Therapy: Determination of Singlet Oxygen Quantum Yield. *Sci Rep* **2016**, *6*, 19954, doi:10.1038/srep19954.
14. Losytskyy, M.; Kuzmenko, L.; Shcherbakov, O.; Gamaleia, N.; Marynin, A.; Yashchuk, V.; Shcherbakov, A. Energy Transfer in Ce0.85Tb0.15F3 Nanoparticles-CTAB Shell-Chlorin E6 System. *Nanoscale Research Letters* **2017**, *12*, 294, doi:10.1186/s11671-017-2077-x.
15. Jang, G.H.; Hwang, M.P.; Kim, S.Y.; Jang, H.S.; Lee, K.H. A Systematic In-Vivo Toxicity Evaluation of Nanophosphor Particles via Zebrafish Models. *Biomaterials* **2014**, *35*, 440–449, doi:10.1016/j.biomaterials.2013.09.054.
16. McCormack, R.N.; Mendez, P.; Barkam, S.; Neal, C.J.; Das, S.; Seal, S. Inhibition of Nanoceria's Catalytic Activity Due to Ce3+ Site-Specific Interaction with Phosphate Ions. *J. Phys. Chem. C* **2014**, *118*, 18992–19006, doi:10.1021/jp500791j.
17. Kim, C.K.; Kim, T.; Choi, I.-Y.; Soh, M.; Kim, D.; Kim, Y.-J.; Jang, H.; Yang, H.-S.; Kim, J.Y.; Park, H.-K.; et al. Ceria Nanoparticles That Can Protect against Ischemic Stroke. *Angewandte Chemie International Edition* **2012**, *51*, 11039–11043, doi:10.1002/anie.201203780.
18. Soh, M.; Kang, D.-W.; Jeong, H.-G.; Kim, D.; Kim, D.Y.; Yang, W.; Song, C.; Baik, S.; Choi, I.-Y.; Ki, S.-K.; et al. Ceria–Zirconia Nanoparticles as an Enhanced Multi-Antioxidant for Sepsis Treatment. *Angewandte Chemie* **2017**, *129*, 11557–11561, doi:10.1002/ange.201704904.
19. Szczeszak, A.; Ekner-Grzyb, A.; Runowski, M.; Szutkowski, K.; Mrówczyńska, L.; Kaźmierczak, Z.; Grzyb, T.; Dąbrowska, K.; Giersig, M.; Lis, S. Spectroscopic, Structural and in Vitro Cytotoxicity Evaluation of Luminescent, Lanthanide Doped Core@shell Nanomaterials GdVO4:Eu3+5%@SiO2@NH2. *Journal of Colloid and Interface Science* **2016**, *481*, 245–255, doi:10.1016/j.jcis.2016.07.025.
20. Runowski, M.; Ekner-Grzyb, A.; Mrówczyńska, L.; Balabhadra, S.; Grzyb, T.; Paczesny, J.; Zep, A.; Lis, S. Synthesis and Organic Surface Modification of Luminescent, Lanthanide-Doped Core/Shell Nanomaterials (LnF3@SiO2@NH2@Organic Acid) for Potential Bioapplications: Spectroscopic, Structural, and in Vitro Cytotoxicity Evaluation. *Langmuir* **2014**, *30*, 9533–9543, doi:10.1021/la501107a.

Preprints (www.preprints.org) | NOT PEER-REVIEWED | Posted: 7 December 2023 doi:10.20944/preprints202312.0494.v1

21. Ansari, A.A.; Parchur, A.K.; Kumar, B.; Rai, S.B. Highly Aqueous Soluble CaF2:Ce/Tb Nanocrystals: Effect of Surface Functionalization on Structural, Optical Band Gap, and Photoluminescence Properties. *J Mater Sci: Mater Med* **2016**, *27*, 178, doi:10.1007/s10856-016-5791-5.
22. Grzyb, T.; Runowski, M.; Szczeszak, A.; Lis, S. Influence of Matrix on the Luminescent and Structural Properties of Glycerine-Capped, Tb3+-Doped Fluoride Nanocrystals. *J. Phys. Chem. C* **2012**, *116*, 17188–17196, doi:10.1021/jp3010579.
23. Ansari, A.A. Influence of Surface Functionalization on Structural and Photo-Luminescence Properties of CeF3:Tb Nanoparticles. *Applied Surface Science* **2017**, *409*, 285–290, doi:10.1016/j.apsusc.2017.03.035.
24. Samanta, T.; Sarkar, S.; Adusumalli, V.N.K.B.; Praveen, A.E.; Mahalingam, V. Enhanced Visible and near Infrared Emissions via Ce3+ to Ln3+ Energy Transfer in Ln3+-Doped CeF3 Nanocrystals (Ln = Nd and Sm). *Dalton Trans.* **2015**, *45*, 78–84, doi:10.1039/C5DT02974K.
25. Wang, J.; Ansari, A.A.; Malik, A.; Syed, R.; Ola, M.S.; Kumar, A.; AlGhamdi, K.M.; Khan, S. Highly Water-Soluble Luminescent Silica-Coated Cerium Fluoride Nanoparticles Synthesis, Characterizations, and In Vitro Evaluation of Possible Cytotoxicity. *ACS Omega* **2020**, *5*, 19174–19180, doi:10.1021/acsomega.0c02551.
26. Dong, H.; Du, S.-R.; Zheng, X.-Y.; Lyu, G.-M.; Sun, L.-D.; Li, L.-D.; Zhang, P.-Z.; Zhang, C.; Yan, C.-H. Lanthanide Nanoparticles: From Design toward Bioimaging and Therapy. *Chem. Rev.* **2015**, *115*, 10725–10815, doi:10.1021/acs.chemrev.5b00091.
27. Shen, X.; Li, T.; Chen, Z.; Geng, Y.; Xie, X.; Li, S.; Yang, H.; Wu, C.; Liu, Y. Luminescent/Magnetic PLGA-Based Hybrid Nanocomposites: A Smart Nanocarrier System for Targeted Codelivery and Dual-Modality Imaging in Cancer Theranostics. *IJN* **2017**, *12*, 4299–4322, doi:10.2147/IJN.S136766.
28. Asadullina, N.R.; Usacheva, A.M.; Smirnova, V.S.; Gudkov, S.V. Antioxidative and Radiation Modulating Properties of Guanosine-5′-Monophosphate. *Nucleosides, Nucleotides & Nucleic Acids* **2010**, *29*, 786–799, doi:10.1080/15257770.2010.518576.
29. Manevich, Y.; Held, K.D.; Biaglow, J.E. Coumarin-3-Carboxylic Acid as a Detector for Hydroxyl Radicals Generated Chemically and by Gamma Radiation. *Radiat Res* **1997**, *148*, 580–591.
30. Wang, Z.L.; Quan, Z.W.; Jia, P.Y.; Lin, C.K.; Luo, Y.; Chen, Y.; Fang, J.; Zhou, W.; O'Connor, C.J.; Lin, J. A Facile Synthesis and Photoluminescent Properties of Redispersible CeF3, CeF3:Tb3+, and CeF3:Tb3+/LaF3 (Core/Shell) Nanoparticles. *Chem. Mater.* **2006**, *18*, 2030–2037, doi:10.1021/cm052360x.
31. Gai, S.; Yang, P.; Li, X.; Li, C.; Wang, D.; Dai, Y.; Lin, J. Monodisperse CeF3, CeF3:Tb3+, and CeF3:Tb3+@LaF3 Core/Shell Nanocrystals: Synthesis and Luminescent Properties. *J. Mater. Chem.* **2011**, *21*, 14610–14615, doi:10.1039/C1JM12419F.
32. Greenhaus, H.L.; Feibush, A.M.; Gordon, Louis. Ultraviolet Spectrophotometric Determination of Cerium(III). *Anal. Chem.* **1957**, *29*, 1531–1534, doi:10.1021/ac60130a045.
33. Malyukin, Y.; Maksimchuk, P.; Seminko, V.; Okrushko, E.; Spivak, N. Limitations of Self-Regenerative Antioxidant Ability of Nanoceria Imposed by Oxygen Diffusion. *J. Phys. Chem. C* **2018**, *122*, 16406–16411, doi:10.1021/acs.jpcc.8b03982.
34. Dutta, P.; Pal, S.; Seehra, M.S.; Shi, Y.; Eyring, E.M.; Ernst, R.D. Concentration of Ce3+ and Oxygen Vacancies in Cerium Oxide Nanoparticles. *Chem. Mater.* **2006**, *18*, 5144–5146, doi:10.1021/cm061580n.
35. Kobashigawa, S.; Kashino, G.; Suzuki, K.; Yamashita, S.; Mori, H. Ionizing Radiation-Induced Cell Death Is Partly Caused by Increase of Mitochondrial Reactive Oxygen Species in Normal Human Fibroblast Cells. *Radiat Res* **2015**, *183*, 455–464, doi:10.1667/RR13772.1.
36. Zhang, B.; Davidson, M.M.; Zhou, H.; Wang, C.; Walker, W.F.; Hei, T.K. Cytoplasmic Irradiation Results in Mitochondrial Dysfunction and DRP1-Dependent Mitochondrial Fission. *Cancer Res* **2013**, *73*, 6700–6710, doi:10.1158/0008-5472.CAN-13-1411.
37. Kawamura, K.; Qi, F.; Kobayashi, J. Potential Relationship between the Biological Effects of Low-Dose Irradiation and Mitochondrial ROS Production. *J Radiat Res* **2018**, *59*, ii91–ii97, doi:10.1093/jrr/rrx091.
38. Waterman, D.P.; Haber, J.E.; Smolka, M.B. Checkpoint Responses to DNA Double-Strand Breaks. *Annu Rev Biochem* **2020**, *89*, 103–133, doi:10.1146/annurev-biochem-011520-104722.
39. Pires, B.R.B.; Silva, R.C.M.C.; Ferreira, G.M.; Abdelhay, E. NF-kappaB: Two Sides of the Same Coin. *Genes* **2018**, *9*, 24, doi:10.3390/genes9010024.
40. Niu, J.; Wang, K.; Kolattukudy, P.E. Cerium Oxide Nanoparticles Inhibits Oxidative Stress and Nuclear Factor-κB Activation in H9c2 Cardiomyocytes Exposed to Cigarette Smoke Extract. *J Pharmacol Exp Ther* **2011**, *338*, 53–61, doi:10.1124/jpet.111.179978.

Preprints (www.preprints.org) | NOT PEER-REVIEWED | Posted: 7 December 2023 doi:10.20944/preprints202312.0494.v1

41. Singh, V.; Gupta, D.; Arora, R. NF-kB as a Key Player in Regulation of Cellular Radiation Responses and Identification of Radiation Countermeasures. *Discoveries (Craiova) 3*, e35, doi:10.15190/d.2015.27.
42. Pesaraklou, A.; Matin, M.M. Cerium Oxide Nanoparticles and Their Importance in Cell Signaling Pathways for Predicting Cellular Behavior. *Nanomedicine* **2020**, *15*, 1709–1718, doi:10.2217/nnm-2020-0104.

Disclaimer/Publisher's Note: The statements, opinions and data contained in all publications are solely those of the individual author(s) and contributor(s) and not of MDPI and/or the editor(s). MDPI and/or the editor(s) disclaim responsibility for any injury to people or property resulting from any ideas, methods, instructions or products referred to in the content.